

Quantum Limitation to the Coherent Emission of Accelerated Charges

A. Angioi and A. Di Piazza*

Max-Planck-Institut für Kernphysik, Saupfercheckweg 1, 69117 Heidelberg, Germany

(Dated: December 5, 2017)

Accelerated charges emit electromagnetic radiation. According to classical electrodynamics if the charges move along sufficiently close trajectories they emit coherently, i.e., their emitted energy scales quadratically with their number rather than linearly. By investigating the emission by a two-electron wave packet in the presence of an electromagnetic plane wave within strong-field QED, we show that quantum effects deteriorate the coherence predicted by classical electrodynamics even if the typical quantum nonlinearity parameter of the system is much smaller than unity, and classical and quantum predictions are expected to agree. We explain this result by observing that coherence effects are also controlled by a new quantum parameter which relates the recoil undergone by the electron with the width of its wave packet in momentum space.

PACS numbers: 12.20.Ds, 41.60.-m

The discovery of techniques such as Chirped Pulse Amplification [1] and Optical Parametric Chirped Pulse Amplification [2] allowed for the development of lasers of increasingly high intensity. Optical pulses with intensities of the order of 10^{22} W/cm² have been already achieved [3] and intensities of the order of 10^{24} W/cm² are envisaged [4, 5]. At such high intensities the interaction between the laser field and an electron (mass m and charge $e < 0$) is highly-nonlinear and electro-dynamical processes involving electrons/positrons occur with the exchange of several photons between laser field and electrons/positrons [6, 7]. This has also primed a surge of interest in testing QED in the so-called “strong-field” regime where the background field intensity is effectively of the order of $\mathcal{I}_{cr} = 4.6 \times 10^{29}$ W/cm², corresponding to the electric field $\mathcal{E}_{cr} = m^2 c^3 / \hbar |e| = 1.3 \times 10^{16}$ V/cm [7]. Due to the Lorentz invariance of the theory, in fact, strong-field QED can be effectively probed at laser intensities $\mathcal{I} \ll \mathcal{I}_{cr}$ by employing ultrarelativistic electron beams with correspondingly high energies $\varepsilon \sim m\sqrt{\mathcal{I}_{cr}/\mathcal{I}} \gg m$ [7]. Indeed, electron beams with energies beyond 1 GeV have been already produced both via conventional [8] and laser-based accelerators [9]. One of the fundamental processes which can be exploited to test strong-field QED is Nonlinear Single Compton Scattering (NSCS), where an electron traveling inside a laser field exchanges multiple photons with the laser field itself while also emitting a single, non-laser photon. NSCS has been studied in the presence of a monochromatic plane wave [6, 10–17], of a pulsed plane wave [18–28], and of a space-time-focused laser beam [29] (see also [30–33]). In [6, 11–15, 17–27] an incoming electron in a plane wave with a definite momentum was investigated, whereas in [16, 28] NSCS by a localized electron wave packet was studied. In all these works, the radiation emitted by a single electron has been considered, such that coherence effects in the nonlinear emission by several electrons have never been investigated within strong-field QED.

In this Letter we explore the novel features in the

quantum radiation spectrum brought about by considering two electron wave packets properly anti-symmetrized as initial state. The generalization to several electrons is straightforward and all new qualitative features are encoded in the two-electron setup. In the single-particle case the spectra calculated quantum mechanically with an incoming electron of definite asymptotic four-momentum p^μ tend to the classical spectra when the quantum nonlinearity parameter $\chi = (kp)\mathcal{E}/m\omega\mathcal{E}_{cr}$ is much smaller than unity [6, 7]. Here, \mathcal{E} , k^μ , and ω are the laser field’s amplitude, its central four-wave-vector, and its central angular frequency, respectively (units with $\hbar = c = 1$ are employed throughout). Now, according to classical physics, if N charges move inside a field along arbitrarily close trajectories, the radiated energy can scale as N^2 (rather than N) up to arbitrarily high frequencies. Below, we consider the paradigmatic case where the two electrons are characterized by the same initial distribution of momenta and, in particular, by the same average quantum parameter χ' . We show that quantum effects limit or completely suppress the coherence of the emission even for $\chi' \ll 1$, i.e., when classical and quantum predictions are expected to agree. We explain this unexpected result by observing that the condition $\chi' \ll 1$ ensures that the typical emitted photon energies are much smaller than the common average energy of electron wave packets. However, coherence effects are also controlled by a new quantum parameter which relates the recoil undergone by the electron not with the average energy but with the width of its wave packet in momentum space.

The laser field is assumed to be linearly polarized and, within the plane-wave approximation, can be described by the classical four-potential $\mathcal{A}_L^\mu(\phi) = (0, \mathcal{A}_L^\mu(\phi)) = \mathcal{A}^\mu \psi_L(\phi)$, where $\psi_L(\phi)$ is a smooth function with compact support and $\phi = (nx)$, with $n^\mu = k^\mu/\omega$. We assume that the plane wave propagates along the positive z direction [$n^\mu = (1, 0, 0, 1)$] and that it is polarized along the x direction [$\mathcal{A}^\mu = (0, -\mathcal{E}/\omega, 0, 0)$]. For the sake of definiteness, we set $\phi = 0$ as the initial light-cone “time” and

thus assume that $\psi_L(\phi) = 0$ for $\phi \leq 0$. We also choose the initial two-electron state as being characterized by two definite spin quantum numbers s_j ($j \in \{1, 2\}$) and having the form

$$|\Psi\rangle = \frac{1}{\sqrt{\mathcal{N}}} \prod_{j=1}^2 \left[\int \frac{d^3 p_j}{(2\pi)^3 \sqrt{2\varepsilon_j}} \rho_j(\mathbf{p}_j) a_{s_j}^\dagger(\mathbf{p}_j) \right] |0\rangle. \quad (1)$$

Here, \mathcal{N} is a normalization factor such that $\langle \Psi | \Psi \rangle = 1$, the operator $a_{s_j}^\dagger(\mathbf{p}_j)$ creates an electron with momentum \mathbf{p}_j (energy $\varepsilon_j = \sqrt{m^2 + \mathbf{p}_j^2}$) and spin quantum number s_j , $\rho_j(\mathbf{p}_j)$ is an arbitrary square-integrable complex-valued function whose modulus square describes the initial momentum distribution of the corresponding electron wave packet, and $|0\rangle$ is the free vacuum state. From the anti-commutation relations $\{a_s(\mathbf{p}), a_{s'}^\dagger(\mathbf{p}')\} = (2\pi)^3 \delta^{(3)}(\mathbf{p} - \mathbf{p}') \delta_{ss'}$ [34], the normalization factor \mathcal{N} turns out to have the form $\mathcal{N} = \mathcal{N}_d - \delta_{s_1 s_2} \mathcal{N}_e$, with

$$\mathcal{N}_d = \int \frac{d^3 p_1}{(2\pi)^3 2\varepsilon_1} \frac{d^3 p_2}{(2\pi)^3 2\varepsilon_2} |\rho_1(\mathbf{p}_1)|^2 |\rho_2(\mathbf{p}_2)|^2, \quad (2)$$

$$\mathcal{N}_e = \int \frac{d^3 p_1}{(2\pi)^3 2\varepsilon_1} \frac{d^3 p_2}{(2\pi)^3 2\varepsilon_2} \rho_1^*(\mathbf{p}_1) \rho_2(\mathbf{p}_1) \rho_2^*(\mathbf{p}_2) \rho_1(\mathbf{p}_2). \quad (3)$$

If $c_{l'}^\dagger(\mathbf{k}')$ is the operator which creates a photon with momentum \mathbf{k}' (energy $\omega' = \sqrt{\mathbf{k}'^2}$) and polarization l' , the final state in NSCS has the form

$$|\Psi'\rangle = \sqrt{8\omega'\varepsilon'_1\varepsilon'_2} c_{l'}^\dagger(\mathbf{k}') a_{s'_2}^\dagger(\mathbf{p}'_2) a_{s'_1}^\dagger(\mathbf{p}'_1) |0\rangle, \quad (4)$$

with $\varepsilon'_j = \sqrt{m^2 + \mathbf{p}'_j{}^2}$. In order to take into account exactly the effects of the plane wave on the electrons' dynamics, we work in the Furry picture [35, 36], where the Dirac field $\Psi(x)$ is expanded with respect to fermion states "dressed" by the classical background plane wave, which are known as Volkov states (see [6, 35, 36] and the Supplemental Material [37]). The leading-order S -matrix element S of NSCS reads

$$S = -ie \int d^4 x \langle \Psi' | \bar{\Psi}(x) \gamma^\mu \Psi(x) A_\mu(x) | \Psi \rangle, \quad (5)$$

where $\bar{\Psi}(x) = \Psi^\dagger(x) \gamma^0$, where γ^μ are the Dirac matrices, and where $A^\mu(x)$ is the quantized part of the electromagnetic field. Here, we neglect the interaction between the electrons as their dynamics is predominantly determined by the intense plane wave.

The calculation of S is straightforward because the corresponding Feynman diagrams are composed of two disconnected pieces (see Fig. 1). At this order of perturbation theory, in fact, only one of the two electrons emits a photon. Now, the orthogonality of Volkov states [6, 20] yields a three-dimensional Dirac (Kronecker) delta-function between the initial and the final

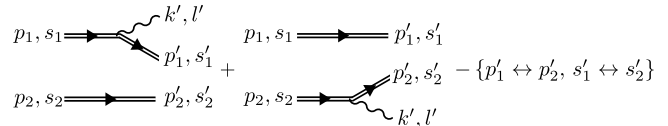


Figure 1. Leading-order Feynman diagrams of NSCS by two electrons. The double lines indicate Volkov states and the symbol $\{p'_1 \leftrightarrow p'_2, s'_1 \leftrightarrow s'_2\}$ indicates the exchange diagrams.

momentum (spin) of non-emitting electrons. Instead, since the plane wave depends on the spacetime coordinates only via $\phi = t - z$, the amplitudes involving the photon emission include a three-dimensional Dirac delta-function, which enforces the conservation of the transverse (\perp) components (x - and y -components) and of the minus ($-$) component (time- minus z -component) of the four-momenta of the involved particles (see also the Supplemental Material). We exploit the altogether six Dirac delta-functions to carry out the six integrals in the initial wave-packet $|\Psi\rangle$ [see Eq. (1)]. Thus, it is convenient to introduce the two on-shell four-momenta q_j^μ ($q_j^2 = m^2$) such that $\mathbf{q}_{j,\perp} = \mathbf{p}'_{j,\perp} + \mathbf{k}'_\perp$ and $q_{j,-} = p'_{j,-} + k'_-$, i.e.,

$$q_j^\mu = p'_{j,\perp}{}^\mu + k'^\mu - \frac{(k'_\perp p'_j)}{p'_{j,-} + k'_-} n^\mu. \quad (6)$$

The amplitude S can be written in the form $S = S_{12} - S_{21}$, where

$$S_{12} = -ie \sqrt{\frac{4\pi}{\mathcal{N}}} \left[\rho_1(\mathbf{q}_1) \rho_2(\mathbf{p}'_2) \delta_{s'_2 s_2} \frac{M_{s'_1 l', s_1}(p'_1, k'; q_1)}{2q_{1,-}} + \rho_1(\mathbf{p}'_1) \rho_2(\mathbf{q}_2) \delta_{s'_1 s_1} \frac{M_{s'_2 l', s_2}(p'_2, k'; q_2)}{2q_{2,-}} \right] \quad (7)$$

and where $S_{21} = S_{12}(p'_1 \leftrightarrow p'_2, q_1 \leftrightarrow q_2, s'_1 \leftrightarrow s'_2)$. Here, we have introduced the reduced amplitude $M_{s' l', s}(p', k'; p)$ characteristic of NSCS by a single electron with definite initial (final) four-momentum p^μ (p'^μ) and spin quantum number s (s'), which emits a photon with four-momentum k' and polarization l' (see, e.g., [21] and the Supplemental Material).

Now, we are interested in the emitted photon energy spectrum $dE_Q/d\omega'$ averaged (summed) with respect to all initial (final) discrete quantum numbers. Since we also integrate over the final electrons momenta, in order to avoid double-counting, we divide the final result by two:

$$\frac{dE_Q}{d\omega'} = \frac{\omega'^2}{8} \sum_{\{s_j s'_j l'\}} \int \frac{d\Omega'}{(2\pi)^3 2} \frac{d^3 p'_1}{(2\pi)^3 2\varepsilon'_1} \frac{d^3 p'_2}{(2\pi)^3 2\varepsilon'_2} |S|^2, \quad (8)$$

where Ω' denotes the solid angle corresponding to $\mathbf{n}' = \mathbf{k}'/\omega'$. Note that if the electrons were distinguishable, the energy emission spectrum would have the same form as in Eq. (8), with the replacement $|S|^2 \rightarrow 2(\mathcal{N}/\mathcal{N}_d)|S_{12}|^2$.

In order to investigate the coherence properties of the emitted radiation, we consider the paradigmatic case in which the two electron wave packets in position space differ only by a translation by a vector \mathbf{r}' , i.e., $\rho_2(\mathbf{p}_2) = \rho_1(\mathbf{p}_2) \exp(-i\mathbf{p}_2 \cdot \mathbf{r}')$, such that $|\rho_1(\mathbf{p})|^2 = |\rho_2(\mathbf{p})|^2$. Also, without loss of generality we choose the function $\rho_1(\mathbf{p}_1)$ to be real and we denote it as $\rho(\mathbf{p}_1)$.

Let us first study the classical energy spectrum $dE_C/d\omega'$ emitted by two electrons in a plane wave [38, 39]

$$\frac{dE_C}{d\omega'} = \frac{e^2\omega'^2}{4\pi^2} \int d\Omega' \left| \sum_{j=1}^2 \int d\phi \frac{p_j'^{\mu}(\phi)}{p_{j,-}'} e^{i\omega'\Phi_j(\phi)} \right|^2. \quad (9)$$

Here, for the sake of notational convenience in relation with the quantum case, we have indicated as $p_j'^{\mu}(\phi) = (\varepsilon_j'(\phi), \mathbf{p}_j'(\phi))$ the electrons' four-momenta in the plane wave [36] (see also the Supplemental Material)

$$p_j'^{\mu}(\phi) = p_j'^{\mu} - e\mathcal{A}_L^{\mu}(\phi) + e \frac{(p_j' \mathcal{A}_L(\phi))}{p_{j,-}'} n^{\mu} - \frac{e^2 \mathcal{A}_L^2(\phi)}{2 p_{j,-}'} n^{\mu}, \quad (10)$$

with initial (at $t = 0$) four-momenta $p_j'^{\mu} = (\varepsilon_j', \mathbf{p}_j')$. Also, by labeling as “1” the electron which first enters the plane wave and by setting the origin of the coordinates system at the corresponding entering point, the initial positions of the electrons are $\mathbf{r}'_1 = \mathbf{0}$ and $\mathbf{r}'_2 = \mathbf{r}'$, with $z' > 0$. The quantity $\Phi_j(\phi)$ thus reads

$$\Phi_j(\phi) = \int_0^{\phi} d\phi' \frac{(n' p_j'(\phi'))}{p_{j,-}'} + \left[\frac{(n' p_j')}{p_{j,-}'} \mathbf{n} - \mathbf{n}' \right] \cdot \mathbf{r}'_j, \quad (11)$$

with $n'^{\mu} = k'^{\mu}/\omega' = (1, \mathbf{n}')$ or $\Phi_j(\phi) = \Phi_j(0) + n'_- \int_0^{\phi} d\phi' [m^2 + \mathbf{P}_{j,\perp}'^2(\phi')]/2p_{j,-}'^2$, where $\mathbf{P}_{j,\perp}'(\phi) = \mathbf{P}_{j,\perp}' - e\mathcal{A}_{L,\perp}(\phi)$, with $\mathbf{P}_{j,\perp}' = \mathbf{p}_{j,\perp}' - p_{j,-}' \mathbf{n}'_{\perp}/n'_-$. Now, by indicating as φ_T a measure of the total laser phase $\omega\phi_T$ where the electrons experience the strong field, an order-of-magnitude condition for the emitted radiation to be coherent is obtained by requiring that $\omega' \Delta\Phi(\phi_T) \lesssim \pi/5$ [40], with $\Delta\Phi(\phi_T) = |\Phi_2(\phi_T) - \Phi_1(\phi_T)|$ (the absolute value of the variation of an arbitrary quantity f is indicated here and below as Δf). Now, we assume that the electrons have initial momenta (energies) of the same order of magnitude \mathbf{p}' (ε'), and that are ultrarelativistic and initially counterpropagating with respect to the laser field ($p'_-/2 \approx \varepsilon' \gg m$). By summing the moduli of all contributions to $\Delta\Phi(\phi_T)$, the above condition provides an upper limit ω'_C on the frequencies which are emitted coherently given by

$$\omega'_C = \frac{2\pi\omega}{5n'_-\varphi_T} \left[\frac{\Delta\overline{\mathbf{P}'^2}}{4\varepsilon'^2} + \frac{\Delta\varepsilon' m^2 + \overline{\mathbf{P}'^2}}{\varepsilon' 2\varepsilon'^2} + \frac{2\omega\Delta\Phi(0)}{n'_-\varphi_T} \right]^{-1}, \quad (12)$$

where $\overline{\mathbf{P}'^2}$ is the average value of $\mathbf{P}'^2(\phi)$ over ϕ_T . It is physically clear that the larger the interaction time

is and the larger the differences in the electrons' initial positions/momenta/energies are, the lower will be the highest frequency that can be emitted coherently.

Having in mind the quantum case where the electrons' momenta distributions are given by $\rho^2(\mathbf{p}'_1)$ and $\rho^2(\mathbf{p}'_2)$, we consider now a classical ensemble of pairs of electrons, each pair being characterized by the electrons' initial positions $\mathbf{r}'_1 = \mathbf{0}$ and $\mathbf{r}'_2 = \mathbf{r}'$ and initial (and final) momenta \mathbf{p}'_j distributed as $\rho^2(\mathbf{p}'_1)$ and $\rho^2(\mathbf{p}'_2)$. The corresponding average classical energy spectrum $\langle dE_C/d\omega' \rangle$ is given by

$$\left\langle \frac{dE_C}{d\omega'} \right\rangle = \int \frac{d^3p'_1}{(2\pi)^3 2\varepsilon'_1} \frac{d^3p'_2}{(2\pi)^3 2\varepsilon'_2} \frac{\rho^2(\mathbf{p}'_1)\rho^2(\mathbf{p}'_2)}{\mathcal{N}_d} \frac{dE_C}{d\omega'}. \quad (13)$$

It is important to observe that this expression can also be obtained from the quantum spectrum $dE_Q/d\omega'$ in Eq. (8) by neglecting the photon recoil in $\rho(\mathbf{q}_j)$, i.e., by approximating $\rho(\mathbf{q}_j) \approx \rho(\mathbf{p}'_j)$, but by keeping linear corrections due to the recoil in the phase of $\rho_2(\mathbf{q}_2)$. This, in fact, allows to reproduce the term $\Phi_2(0)$ from the difference $\mathbf{q}_2 - \mathbf{p}'_2$ according to Eq. (6) after neglecting higher-than-linear recoil terms in it. On the one hand, this observation indicates that when the photon recoil is negligible, the classical constraint in Eq. (12) also applies quantum mechanically. On the other hand, however, we will show below that the differences in the coherence properties of classical and quantum radiation precisely arise from the fact that the classical theory ignores the recoil in $\rho(\mathbf{q}_j)$. In fact, turning now to the quantum case, it is intuitively clear, as we have also ascertained in the numerical example below, that the electrons' indistinguishability does not play a significant role here. Indeed, the exchange terms become important only when the two electrons have very similar final momenta (and the same final spin), which corresponds to a negligibly small region of the available final phase space. Thus, in order to study coherence effects, we focus on the interference term in $|S_{12}|^2$, which is proportional to the product $\rho(\mathbf{q}_1)\rho(\mathbf{p}'_1)\rho(\mathbf{p}'_2)\rho(\mathbf{q}_2)$ [see Eq. (7)]. In analogy with the classical case, we indicate as \mathbf{p}' the average momentum of both electron distributions, corresponding to the on-shell four-momentum $p'^{\mu} = (\varepsilon', \mathbf{p}') = (\sqrt{m^2 + \mathbf{p}'^2}, \mathbf{p}')$, and as $\sigma_{\mathbf{p}'}$ the three-dimensional width. As it is clear from Eq. (6), the difference between the momenta \mathbf{p}'_j and \mathbf{q}_j is due to the photon recoil. Thus, if the latter is so large that $|p'_{j,i} - q_{j,i}| \gg \sigma_{p_i}$ for any $i \in \{x, y, z\}$, the interference term will be suppressed because the functions $\rho(\mathbf{q}_j) = \rho(\mathbf{q}_j(\mathbf{p}'_j))$ [see Eq. (6)] and $\rho(\mathbf{p}'_j)$ cannot be both significantly different from zero for the same \mathbf{p}'_j . Notice that the fact that two functions $\rho(\mathbf{p})$ and $\rho(\mathbf{p} + \delta\mathbf{p})$ overlap or not does not depend on the frame of reference. As a result, the interference term in $|S_{12}|^2$ will be suppressed and the radiation with frequency $\omega' \gtrsim \omega'_Q = \min_i \{\sigma_{p'_i}/|\cos\theta'_i|\}$, with θ'_i being the angle between \mathbf{k}' and the i th axis, will be incoherent [the

last term in Eq. (6) has been neglected, which is a good approximation in most situations of interest]. The additional quantum restriction to the coherent emission of radiation is qualitatively different from the classical one and it can be related to the particles' "kinematic" indistinguishability. In fact, depending on the width of the electron wave packets, even a perfect knowledge of the final momenta of the two electrons and of the emitted photon combined with the momentum conservation laws does not allow to know with certainty which electron has emitted the photon. In this respect, different momentum components of the two-electron wave packet $|\Psi\rangle$ constructively interfere enhancing the radiation probability. This is in striking contrast with the case of an incoming single electron, where, indeed, the conservation laws allow to determine the initial momentum of the electron once the final electron and photon momenta are known, implying that the emission spectrum is given by the incoherent sum of the emissions spectra corresponding to each momentum component of the wave packet [16, 28].

Below, we show by means of a numerical example that the quantum restriction to the coherence of the emission can be essentially more restrictive than the classical one even in the striking case where the average quantum parameter $\chi' = (kp')\mathcal{E}/m\omega\mathcal{E}_{cr}$ of the two wave packets is much smaller than unity. To do this we compare in Fig. 2 the full quantum spectrum $dE_Q/d\omega'$ from Eq. (8) (solid black line) with the classical spectrum $\langle dE_C/d\omega' \rangle$ from Eq. (13) (dash-dotted red line). Since the distributions of the momenta of the two electrons are the same, the two single-particle spectra are identical [28]. Thus, as references to discuss coherence effects, we also show these single-electron spectra multiplied by two (dashed green line) and by four (dotted blue line). Concerning the electrons, we have set the function $\rho^2(\mathbf{p}'_j)/2\varepsilon'_j$ to be a normalized Gaussian function, with average momentum $\mathbf{p}' = (0, 0, -100 \text{ MeV})$, transverse standard deviation $\sigma_{p'_x} = \sigma_{p'_y} = \sigma_{p'_z} = 1 \text{ keV}$, and longitudinal standard deviation $\sigma_{p'_\parallel} = \sigma_{p'_z}$ indicated in each panel of the figure. In order to have a non-negligible interference term, we have chosen the components of the vector \mathbf{r}' to be smaller than the corresponding wave packet "size" $1/\sigma_{p'_i}$: $\mathbf{r}' = (0, 10^{-4} \text{ eV}^{-1}, 10^{-7} \text{ eV}^{-1})$. We have ensured that the spectra in Fig. 2 do not change significantly with \mathbf{r}' as long as $|\mathbf{r}' \cdot \boldsymbol{\sigma}_{p'}| \ll 1$, with the exception of the classical spectra, where oscillations due to classical interference may appear. Concerning the plane wave, we have set $\omega = 1.55 \text{ eV}$, $\mathcal{I} = 1.2 \times 10^{21} \text{ W/cm}^2$, and $\psi_L(\phi) = \sin^4(\omega\phi/4) \sin(\omega\phi)$ for $0 \leq \omega\phi \leq 4\pi$ and zero elsewhere. With these parameters it is $\chi' \approx 0.02$, thus the classical and the quantum single-particle spectra emitted by each electron wave packet are very similar and do not depend strongly on $\sigma_{p'_\parallel}$ [28].

Fig. 2 shows that the classical spectra (dash-dotted red lines) are coherent up to a given frequency, which

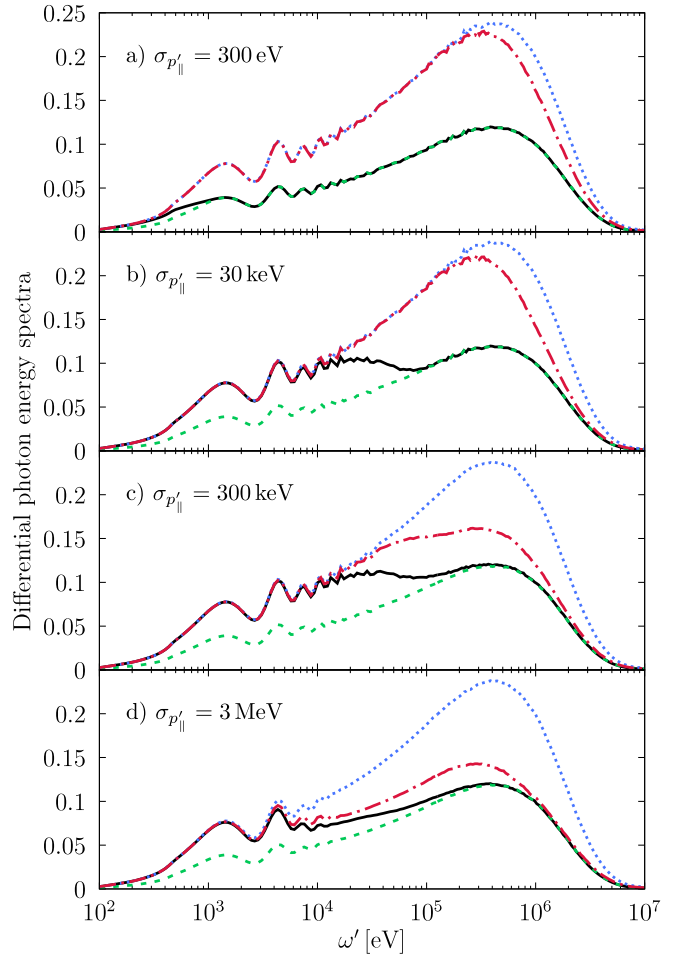


Figure 2. (Color online) Emitted energy spectra for the numerical parameters given in the text. The solid black line shows the quantum spectrum $dE_Q/d\omega'$ and the dash-dotted red line shows the classical spectrum $\langle dE_C/d\omega' \rangle$. As reference, the corresponding single-electron spectrum multiplied by two (dashed green line) and by four (dotted blue line) are also shown.

depends on $\sigma_{p'_\parallel}$. In order to predict the value of this frequency from Eq. (12), we choose $\mathbf{n}' \sim (m\xi/2\varepsilon', 0, -1)$, with $\xi = |e|\mathcal{E}/m\omega \approx 17 \ll \varepsilon'/m \approx 200$, as a typical observation direction where the average radiated energy is large [21] and we estimate the variations $\Delta\mathbf{p}'_\perp$ and $\Delta\varepsilon' \approx \Delta p'_\parallel$ entering Eq. (12) as the standard deviations $\sqrt{2}\sigma_{p'_\perp}$ and $\sqrt{2}\sigma_{p'_\parallel}$, respectively, of the differences between the components of the two random variables \mathbf{p}'_1 and \mathbf{p}'_2 . By also estimating $\Delta\Phi(0) \approx |\mathbf{n}' \cdot \mathbf{r}'| \sim z'$, and $\varphi_T \sim 2\pi$ as the effective phase where the laser field is strong, we find from Eq. (12) that ω'_C is $4.6 \times 10^5 \text{ eV}$ for $\sigma_{p'_\parallel} = 300 \text{ eV}$, $1.6 \times 10^5 \text{ eV}$ for $\sigma_{p'_\parallel} = 30 \text{ keV}$, $2.4 \times 10^4 \text{ eV}$ for $\sigma_{p'_\parallel} = 300 \text{ keV}$, and $2.5 \times 10^3 \text{ eV}$ for $\sigma_{p'_\parallel} = 3 \text{ MeV}$, in good agreement with the numerical results in Fig. 2, accounting for the simplicity of the analytical model. Instead, the quantum spectra (solid black lines) show that

the emission is coherent on a significantly smaller frequency region. In fact, by estimating $|\mathbf{k}'_{\perp}| \sim \omega' m \xi / \varepsilon'$, we obtain that $\omega'_Q \sim \min\{\sigma_{p'_{\perp}} \varepsilon' / m \xi, \sigma_{p'_{\parallel}}\}$, which corresponds to $\sigma_{p'_{\parallel}} = 3 \times 10^2 \text{ eV}$ in the case of panel a), and to $\sigma_{p'_{\perp}} \varepsilon' / m \xi = 1.2 \times 10^4 \text{ eV}$ in the other cases. This prediction is also confirmed by the numerical results. In particular, it is interesting to observe the interplay between the classical and the quantum upper limits, with the latter dominating in panels a)-c) where $\omega'_C > \omega'_Q$ and the former taking over in panel d) where $\omega'_C < \omega'_Q$.

The properties of single-electron pulses with energies of the order of 100 keV are already exploited experimentally in order to perform high-precision spectroscopy (see [41] and references therein). Moreover, recent theoretical studies indicate the feasibility of generating single-electron wave packets with GeV energies [42]. The extension to few-electron beams seems already feasible and our results suggest that the development of similar techniques at higher energies would have important applications also in fundamental strong-field physics. By reverting the argument, we can also say that the NSCS spectra as calculated here can be exploited, provided a detailed knowledge of the laser pulse, as a diagnostic tool for two- or few-electron high-energy pulses.

In conclusion, we have shown that in the process of emission of radiation by a system of two electrons, classical predictions can significantly differ from the quantum ones even when the typical quantum nonlinearity parameter of the system is much smaller than unity. In fact, a qualitative new limit arises quantum mechanically on the frequencies which can be emitted coherently as compared to classical electrodynamics. We have shown that this limit depends on the ratio between the photon recoil and the width of the electron wave packets in momentum space.

The authors would like to acknowledge K. Z. Hatsagortsyan and J. Evers for helpful discussions. A. A. is also thankful to S. Bragin, S. Castrignano, S. M. Cavalletto, and O. D. Skoromnik for the feedback they provided during the development of the ideas contained in this paper.

* dipiazza@mpi-hd.mpg.de

- [1] D. Strickland and G. Mourou, *Opt. Commun.* **56**, 219 (1985).
- [2] A. Piskarskas, A. Stabinis, and A. Yankauskas, *Phys. Usp.* **29**, 869 (1986).
- [3] V. Yanovsky, V. Chvykov, G. Kalinchenko, P. Rousseau, T. Planchon, T. Matsuoka, A. Maksimchuk, J. Nees, G. Chériaux, G. Mourou, and K. Krushelnick, *Opt. Express* **16**, 2109 (2008).
- [4] Extreme Light Infrastructure (ELI), <http://www.eli-laser.eu/>, (2017).
- [5] Exawatt Center for Extreme Light Studies (XCELS), <http://www.xcels.iapras.ru/>, (2017).
- [6] V. I. Ritus, *J. Sov. Laser Res.* **6**, 497 (1985).
- [7] A. Di Piazza, C. Müller, K. Z. Hatsagortsyan, and C. H. Keitel, *Rev. Mod. Phys.* **84**, 1177 (2012).
- [8] C. Patrignani *et al.* (Particle Data Group), *Chin. Phys. C* **40**, 100001 (2017).
- [9] W. P. Leemans, A. J. Gonsalves, H.-S. Mao, K. Nakamura, C. Benedetti, C. B. Schroeder, C. Tóth, J. Daniels, D. E. Mittelberger, S. S. Bulanov, J.-L. Vay, C. G. R. Geddes, and E. Esarey, *Phys. Rev. Lett.* **113**, 245002 (2014).
- [10] I. I. Goldman, *Phys. Lett.* **8**, 103 (1964).
- [11] L. S. Brown and T. W. B. Kibble, *Phys. Rev.* **133**, A705 (1964).
- [12] A. I. Nikishov and V. I. Ritus, *Sov. Phys. JETP* **19**, 529 (1964).
- [13] Z. Fried and J. H. Eberly, *Phys. Rev.* **136**, B871 (1964).
- [14] D. Y. Ivanov, G. L. Kotkin, and V. G. Serbo, *Eur. Phys. J. C* **36**, 127 (2004).
- [15] C. Harvey, T. Heinzl, and A. Ilderton, *Phys. Rev. A* **79**, 063407 (2009).
- [16] J. P. Corson, J. Peatross, C. Müller, and K. Z. Hatsagortsyan, *Phys. Rev. A* **84**, 053831 (2011).
- [17] T. N. Wistisen, *Phys. Rev. D* **90**, 125008 (2014).
- [18] M. Boca and V. Florescu, *Phys. Rev. A* **80**, 053403 (2009).
- [19] T. Heinzl, D. Seipt, and B. Kämpfer, *Phys. Rev. A* **81**, 022125 (2010).
- [20] M. Boca and V. Florescu, *Eur. Phys. J. D* **61**, 449 (2011).
- [21] F. Mackenroth and A. Di Piazza, *Phys. Rev. A* **83**, 032106 (2011).
- [22] D. Seipt and B. Kämpfer, *Phys. Rev. A* **83**, 022101 (2011).
- [23] V. Dinu, T. Heinzl, and A. Ilderton, *Phys. Rev. D* **86**, 085037 (2012).
- [24] M. Boca, V. Dinu, and V. Florescu, *Phys. Rev. A* **86**, 013414 (2012).
- [25] V. Dinu, *Phys. Rev. A* **87**, 052101 (2013).
- [26] K. Krajewska, M. Twardy, and J. Z. Kamiński, *Phys. Rev. A* **89**, 052123 (2014).
- [27] A. I. Titov, B. Kämpfer, T. Shibata, A. Hosaka, and H. Takabe, *Eur. Phys. J. D* **68**, 299 (2014).
- [28] A. Angioi, F. Mackenroth, and A. Di Piazza, *Phys. Rev. A* **93**, 052102 (2016).
- [29] A. Di Piazza, *Phys. Rev. A* **95**, 032121 (2017).
- [30] A. Di Piazza, *Phys. Rev. Lett.* **113**, 040402 (2014).
- [31] A. Di Piazza, *Phys. Rev. A* **91**, 042118 (2015).
- [32] T. Heinzl and A. Ilderton, *Phys. Rev. Lett.* **118**, 113202 (2017).
- [33] T. Heinzl and A. Ilderton, *J. Phys. A* **50**, 345204 (2017).
- [34] M. E. Peskin and D. V. Schroeder, *An Introduction to Quantum Field Theory* (Addison-Wesley, Reading, 1995).
- [35] W. H. Furry, *Phys. Rev.* **81**, 115 (1951).
- [36] V. Berestetskii, E. Lifshitz, and L. Pitaevskii, *Quantum Electrodynamics* (Butterworth-Heinemann, Oxford, 1982).
- [37] See Supplemental Material for an expression of the positive-energy Volkov states and other well-known textbook results.
- [38] J. D. Jackson, *Classical electrodynamics*, 3rd ed. (Wiley, New York, 1999).
- [39] V. N. Baier, V. M. Katkov, and V. M. Strakhovenko, *Electromagnetic processes at high energies in oriented*

single crystals (World Scientific, Singapore, 1998).

- [40] This condition is obtained starting from the prototype function $g(\theta) = |1 + \exp(i\theta)|^2$ and by stating that it shows a “coherent” behavior for $\theta < \theta^*$, where θ^* is such that $|g(\theta^*) - 4|/4 = 0.1$, i.e. $\theta^* \approx \pi/5$.
- [41] P. Baum, Chem. Phys. **423**, 55 (2013).
- [42] K. Krajewska, F. Cajiao Vélez, and J. Z. Kamiński, Proc. SPIE **10241**, 102411J (2017).

Quantum Limitation to the Coherent Emission of Accelerated Charges: Supplemental Material

A. Angioi and A. Di Piazza*

Max-Planck-Institut für Kernphysik, Saupfercheckweg 1, 69117 Heidelberg, Germany

PACS numbers: 12.20.Ds, 41.60.-m

In the present Supplemental Material we provide some results that we did not include in the main text because they are widely known in the literature (see e.g. [1–3]). For the sake of clarity the numbers of the equations here contain “SM” in addition, such that the usual numbering (without SM) refers to the equations in the main text.

VOLKOV STATES

As we mentioned in the main text, our work is carried out in the Furry picture [1]. Thus, the fermion field $\Psi(x)$ in Eq. (5) needs to be expanded by employing “dressed” electron states, i.e., the solutions of the Dirac equation in the background field. In our case the background field is a linearly-polarized plane wave described by the four-vector potential $\mathcal{A}_L^\mu(\phi) = \mathcal{A}^\mu \psi_L(\phi)$, where $\psi_L(\phi)$ is a smooth function with compact support, with $\phi = (nx) = t - z$, i.e., $n^\mu = (1, 0, 0, 1)$ [see also the main text above Eq. (1) for additional details], and the resulting solutions of the Dirac are the so-called Volkov states [1]. By setting $\phi = 0$ as the initial light-cone “time” and by correspondingly assuming that $\psi_L(\phi) = 0$ for $\phi \leq 0$, the positive-energy Volkov state of an electron with four-momentum p^μ and a spin quantum number s at $\phi = 0$ reads

$$\psi_{ps}(x) = \left[1 + \frac{e}{2p_-} \not{n} \mathcal{A}_L(\phi) \right] u_{ps} e^{iS_p(x)}. \quad (\text{SM.1})$$

Here, we have introduced the minus-component $p_- = (np)$, the “slash” notation $\not{v} = \gamma^\mu v_\mu$ for an arbitrary four-vector v^μ , with γ^μ being the Dirac gamma-matrices, the constant bispinor u_{ps} fulfilling $(\not{p} - m)u_{ps} = 0$ and normalized as $\bar{u}_{ps}u_{ps} = 2m$ [1], and the classical action $S_p(x)$ of the electron in the plane wave

$$S_p(x) = -(px) - \int_0^\phi d\phi' \left[\frac{e(p\mathcal{A}_L(\phi'))}{p_-} - \frac{e^2 \mathcal{A}_L^2(\phi')}{2p_-} \right]. \quad (\text{SM.2})$$

It is possible to associate the average four-current

$$j_p^\mu(\phi) = \frac{\bar{\psi}_{ps}(x) \gamma^\mu \psi_{ps}(x)}{\bar{\psi}_{ps}(x) \psi_{ps}(x)} \quad (\text{SM.3})$$

to the Volkov state $\psi_{ps}(x)$ and it turns out that $j_p^\mu(\phi) = p^\mu(\phi)/m$, where $p^\mu(\phi) = (\varepsilon(\phi), \mathbf{p}(\phi))$ is the solution of

the Lorentz equation in the plane wave with initial four-momentum p^μ :

$$p^\mu(\phi) = p^\mu - e\mathcal{A}_L^\mu(\phi) + n^\mu \left[e \frac{(p\mathcal{A}_L(\phi))}{p_-} - \frac{e^2 \mathcal{A}_L^2(\phi)}{2p_-} \right]. \quad (\text{SM.4})$$

NONLINEAR SINGLE COMPTON SCATTERING

The leading order S -matrix element S_{fi} of nonlinear single Compton scattering by an electron with initial (final) four-momentum p^μ (p'^μ) and spin quantum number s (s') is given within the Furry picture by

$$S_{fi} = -ie\sqrt{4\pi} \int d^4x \bar{\psi}_{p's'}(x) \not{\epsilon}'_{l'} e^{i(k'x)} \psi_{ps}(x), \quad (\text{SM.5})$$

where k'^μ is the four-momentum of the emitted photon and $\epsilon'_{l'}^\mu$ its polarization four-vector, with $l' \in \{1, 2\}$. Since the integrand in Eq. (SM.5) depends non-trivially only on $\phi = t - z$, the remaining three spacetime integrals provide corresponding momenta delta-functions and S_{fi} can be written in the form

$$S_{fi} = -ie\sqrt{4\pi}(2\pi)^3 \delta^{(x,y,-)}(p - k' - p') M_{s'l',s}(p', k'; p). \quad (\text{SM.6})$$

By recalling the matrix structure of Volkov states [see Eq. (SM.1)], the reduced amplitude $M_{s'l',s}(p', k'; p)$ can be written as $M_{s'l',s}(p', k'; p) = \bar{u}_{p's'} \tilde{M}_{l'}(p', k'; p) u_{ps}$, with [3]

$$\begin{aligned} \tilde{M}_{l'}(p', k'; p) = & \not{\epsilon}'_{l'} f_0 + e \left(\frac{\not{A} \not{\epsilon}'_{l'}^*}{2p'_-} + \frac{\not{\epsilon}'_{l'}^* \not{A}}{2p_-} \right) f_1 \\ & - \frac{e^2 \mathcal{A}^2 \not{\epsilon}'_{l'}^*}{2p_- p'_-} f_2, \end{aligned} \quad (\text{SM.7})$$

where

$$f_b = \int d\phi \psi_L^b(\phi) e^{i \int_0^\phi d\phi' [a_0 + a_1 \psi_L(\phi') + a_2 \psi_L^2(\phi')]}, \quad (\text{SM.8})$$

with $b \in \{0, 1, 2\}$ and

$$a_0 = \frac{(k'p)}{p'_-}, \quad (\text{SM.9})$$

$$a_1 = \frac{e(p'A)}{p'_-} - \frac{e(pA)}{p_-}, \quad (\text{SM.10})$$

$$a_2 = -\frac{e^2 \mathcal{A}^2}{2} \frac{k'_-}{p_- p'_-}. \quad (\text{SM.11})$$

Note that, by either enforcing gauge invariance or by integrating it by parts, the formally divergent integral f_0 can be regularized according to the identity $f_0 = -(a_1 f_1 + a_2 f_2)/a_0$ [3].

CLASSICAL LIMIT

In order to make the classical limit mentioned below Eq. (13) more transparent, we notice that in the single-electron case considered here:

1. by neglecting the recoil in Eq. (SM.7), i.e., by approximating $p'_- \approx p_-$ there and $u_{p's'} \approx u_{ps'}$, the pre-exponential of the matrix $M_{s'l',s}(p',k';p)$ reduces to $2(p(\phi)\epsilon'_{l'})\delta_{ss'}$;
2. by neglecting terms higher than linear in the pho-

ton recoil in the coefficients a_0 , a_1 and a_2 , i.e., by approximating $a_0 \approx (k'p)/p_-$, $a_1 \approx e[p_-(k'\mathcal{A}) - k'_-(p\mathcal{A})]/p_-^2$, and $a_2 \approx -e^2\mathcal{A}^2k'_-/2p_-^2$, the phase of the integrands in the functions f_b coincides with the corresponding classical phase in Eq. (9) (for an electron in the origin at $t = 0$).

* dipiazza@mpi-hd.mpg.de

- [1] V. B. Berestetskii, E. M. Lifshitz, and L. P. Pitaevskii, *Quantum Electrodynamics* (Elsevier, Oxford, 1982).
- [2] V. N. Baier, V. M. Katkov, and V. M. Strakhovenko, *Electromagnetic Processes at High Energies in Oriented Single Crystals*, (World Scientific, Singapore, 1998).
- [3] F. Mackenroth and A. Di Piazza, Phys. Rev. A **83**, 032106 (2011).